ACS Catalysis

Letter

pubs.acs.org/acscatalysis

Understanding Tantalum-Catalyzed Ethylene Trimerization: When Things Go Wrong

Yin Chen,[†] Raffaele Credendino,[†] Emmanuel Callens,[†] Muhammad Atiqullah,[‡] Mamdouh A. Al-Harthi,[§] Luigi Cavallo,[†,*] and Jean-Marie Basset[†,*]

[†]Kaust Catalysis Center, Physical Sciences and Engineering, King Abdullah University of Science and Technology (KAUST), Thuwal 23955-6900, Saudi Arabia

[‡]Center for Refining & Petrochemicals (CRP) and Center of Research Excellence in Petroleum Refining & Petrochemicals (CoRE-PRP), King Fahd University of Petroleum & Minerals, Dhahran 31261, Saudi Arabia

[§]Department of Chemical Engineering, King Fahd University of Petroleum & Minerals, Dhahran 31261, Saudi Arabia

Supporting Information

ABSTRACT: Ethylene oligomerization to linear low-molecular-mass α-olefins is an open industrial challenge. Ta-based catalysts are promising systems, but the unclear understanding of their behavior prevents systematic advances in the field. We demonstrate here that a well-defined $(\equiv SiO)_3Ta^{III}$ species is able to promote ethylene oligo-/polymerization without any cocatalyst, confirming that the active species in Ta systems corresponds to a Ta^{III} species. DFT calculations on a series of Ta systems ranging from ethylene trimerization to ethylene polymerization catalysts highlight the key factors controlling their experimental behavior. Comparison of these Ta systems allows one to set general rules for the rational development of new ethylene Ta oligomerization catalysts.

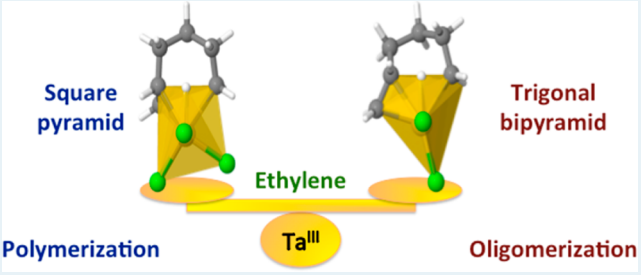

KEYWORDS: *Heterogeneous catalysis, Ethylene oligomerization, Ethylene polymerization, Tantalum catalysis, Surface organometallic chemistry*

During recent decades, scientists have been able to trigger consecutive addition of thousands of ethylene and propylene molecules to a transition metal−carbon bond, leading to high-molecular-mass polymers (principally polyethylene (PE) and polypropylene (PP)).[1] This achievement has also been possible because of the great understanding of the various factors controlling the kinetic competition between the chain growth reaction and the most challenging chain release/transfer reactions, typically β-H transfer to either the monomer or the metal, or chain transfer to the cocatalyst.[2] This has enhanced the development of the catalysts and the field of selective ethylene oligomerization. Yet, the selective production of low-molecular-weight, C8−C20 linear α-olefins (LAOs) remains a challenge.[3] To date, mainly Ti and Cr catalyst systems are playing a leading role in industry,[4] and only recently have Ta catalysts emerged as a promising alternative.[5,6]

Focusing on the Ta-based catalysts for ethylene oligomerization, Sen et al. showed that using an alkylating agent, $TaCl_5$ produces highly branched polyethylene as a result of the copolymerization of ethylene and the in situ generated oligomers.[5a] In addition, they found that $TaCl_5$ could selectively trimerize ethylene to 1-hexene with moderate activity by changing the alkylating reagent.[6a] They postulated that a Ta^{III} species reduced from $Ta^{V}Me_2Cl_3$ under ethylene atmosphere is the active species. The DFT calculations by Houk and Yu using $TaCl_3$, **1**, as a model of the active species also supported this hypothesis and demonstrated the viability of tantalacycloalkanes as intermediates in the trimerization process.[7] In this context, Mashima et al. alternatively generated a Ta^{III} active species formed by reduction of $TaCl_5$ with 3,6-bis-(trimethylsilyl)-1,4-cyclohexadiene derivatives.[6b] Using NMR spectroscopy, they have shown a Ta-metallacycle as the reaction medium.

Recently, we reported that $(\equiv SiO)Ta^{V}Me_2Cl_2$, **2**, formed by grafting $TaMe_3Cl_2$ on a partially dehydroxylated SBA-15, is an effective ethylene trimerization catalyst that, surprisingly and unlike the previous tantalum systems, needs no cocatalyst.[8] Monitoring the activation period with this well-defined $(\equiv SiO)Ta^{V}Cl_2Me_2$ system enabled us to demonstrate that ethylene initially converts the Ta^{V} catalyst precursor into a putative reduced Ta^{III} species, which can then generate the key metallacycle intermediates. Consequently, by comparison with the previously mentioned systems, the good performance of this catalyst indicated that replacing a chloride ligand by a surface bulky siloxy and also by immobilization on a rigid support did not diminish trimerization efficiency, which we

Received: May 12, 2013
Published: May 17, 2013

   dx.doi.org/10.1021/cs400349p | ACS Catal. 2013, 3, 1360−1364

recall as an extremely delicate balance between chain growth and chain release/transfer kinetics.

In all the above Ta^{V} catalysts, the real active species is a putative Ta^{III} intermediate with only indirect experimental support, due to the well-known high instability of Ta^{III} species.[9] To unequivocally demonstrate this hypothesis, we decided to evaluate the performance of a solid surface stable Ta^{III} species, namely, $(\equiv SiO)_3Ta$, **3**. This compound was previously obtained by thermal treatment of the alkane metathesis catalyst $(\equiv SiO)_2TaH$ under hydrogen and characterized by EXAFS.[10,11] Reaction with pent-2-yne also confirmed the formation of tantalum(III) species (see the Supprting Information (SI)).[9] We anticipated from the previous reasoning that **3** would catalyze ethylene oligomerization (preferably trimerization). Unexpectedly, experiments indicated that **3** is efficient for ethylene polymerization.

Therefore, applying a combined experimental and theoretical approach, we decided to compare the experimentally characterized systems **1**−**3**, to unambiguously confirm that Ta^{III} is the active species and to explain why the reaction is switching from selective ethylene trimerization to polymerization. The model adopted for **2** is shown in Figure 1. Two

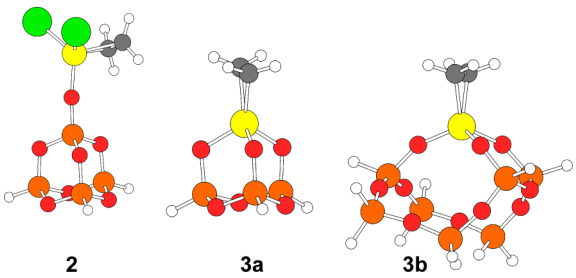

Figure 1. Ethylene coordinated geometries of the silica-grafted Ta catalysts studied by DFT.

geometries were considered for **3** in the calculations, **3a** and **3b** of Figure 1, because different species can be envisaged for a tripodal Ta grafted on silica; see the SI for further information. Since all the optimized geometries of the key transition states based on **3a** and **3b** present two O−Si−O angles close 90° and the third varying in the 90°−110° range, we extended the analysis to two hypothetical $TaCl_3$ species: one with the three Cl−Ta−Cl angles fixed at 90°, **4a**; the other, with two angles fixed at 90°; and the third, at 110°, **4b**.

Initially, we investigated the reactivity of catalyst **3** toward ethylene (for synthesis, elemental analysis, and other characterization, see the SI). The reaction was conducted using **3** directly in the presence of ethylene (Table 1, entry 1). At the end of the reaction, we isolated PE as the main product with trace amounts of oligomers, such as 1-butene and 1-hexene. In the presence of toluene, PE was still obtained as the main product, with an increased amount of various C_4−C_{24} oligomers. Comparison of entries 2−7 in Table 1 indicates that temperature strongly influences product distribution and overall productivity. PE production reached a maximum at 70 °C, with a polymerization activity of 85.6 $kg_{PE}/mol_{Ta}\cdot h$ at 50 bar(g) of ethylene. Lower ethylene pressure leads to a decrease in PE production (Table 1, entries 4, 8−11). We also observed $(\equiv SiO)_2TaH_x$ is not reactive for ethylene polymerization at all (Table 1, entries 4, 12).

^{1}H NMR and ^{13}C NMR spectroscopies are consistent with a linear backbone of the synthesized PEs (SI Figures S10, S11),

Table 1. Oligo- versus Polymerization of Ethylene Catalyzed by 3

entry[a]	P (bar (g))	T (°C)	1-butene (mg)	1-hexene (mg)	PE (g)	productivity[b] ($kg_{PE}/mol_{Ta}\cdot h$)
1[c]	50	70			1.51	58.5
2	50	100	trace	18	0.56	43.4
3	50	85	trace	19	0.74	57.4
4	50	70	10	27	1.10	85.6
5	50	55	15	37	0.57	44.4
6	50	40	20	47	0.50	38.4
7	50	25	15	34	0.33	24.4
8	40	70	trace	30	1.06	82.2
9	30	70	trace	26	0.95	73.7
10	20	70	trace	25	0.56	42.5
11	10	70	trace	21	0.36	27.5
12[d]	50	70			0.05	

[a]Reaction conditions: 25 mg (13 μmol of Ta) of catalyst **3** with 5 mL of toluene in a semibatch autoclave for 1 h. [b]Productivity of PE. [c]The reaction was carried out in gas phase without toluene, and 50 mg catalyst **3** was used. [d]50 mg $(\equiv SiO)_2TaH_x$ was used without solvent.

whereas DSC analysis indicates peak melting temperatures (T_{pm}s) of 127.96−130.52 °C. The corresponding polymer densities are ~0.944 g/cm^3. The peak melting temperature and density values are typical of linear PEs. The formation of a linear backbone is also attested by the successive self-nucleation and annealing (SSA) DSC experiments (SI Figure S12, S13). GPC analysis of the PE samples, synthesized using toluene at different pressures, shows very high weight-average molecular masses ($\bar{M}_w$) of 9.43×10^5 and 1.11×10^6 g/mol, respectively, with very broad molecular mass distributions ($\bar{M}_w/\bar{M}_n$) of 270.0 and 346.7 (Table 2), indicative of the presence of different Ta

Table 2. Molecular Masses and Molecular Mass Distribution of the PEs Produced by 3

sample[a]	$\bar{M}_w$[c]	$\bar{M}_n$[c]	$\bar{M}_w/\bar{M}_n$
1 (entry 8, table 1)[b]	9.43×10^5	3442	270.0
2 (entry 4, table 1)[c]	1.11×10^6	3923	292.2

[a]PE produced using slurry polymerization in toluene. [b]Average of two runs. [c]Units: g/mol.

species active in polymerization. This is also consistent with ^{31}P CP MAS spectroscopy displaying a broad peak, which indicates the presence of multiple tripodal Ta species on the silica surface (see SI Figure S7). The extreme rectangular part of the Crystaf analysis shows the formation of nonvolatile oligomers in samples 1 and 2 of Table 2, with temperature peaks of 87 °C for sample 1 and 85.5 and 90.2 °C for sample 2, representative of linear PE. In addition, the observed ultrahigh molecular mass PE by GPC is in agreement with the absence of an alkylating cocatalyst, which acts as a chain-transfer agent that eventually reduces the molecular mass.

GC analysis indicates that the low-mass fraction is composed of LAOs in the range C4−C24 with an even number of C atoms (traces of branched isomers are detected). The absence of alkanes indicates that oligomers are formed through typical β-H transfer. The distribution of the oligomers is not a typical Schulz−Flory behavior. (see SI Figure S9). In addition, in situ analysis of the effluent gas, from catalyst **3** under a diluted ethylene flow in a fixed bed reactor (1 bar, 20 °C, 20 mL/min, He/C_2H_4 = 8:1), indicated that only 1-butene and 1-hexene are

dx.doi.org/10.1021/cs400349p | ACS Catal. 2013, 3, 1360−1364

generated. After 4 h, an increase in the pressure in the reactor was observed as a result of the formation of PE. As expected, analysis of the data reported in Table 1 entries 2−6 shows that the 1-hexene amount inversely correlates to the PE yield.

Overall, the above results show that species **3** is an ethylene oligo-/polymerization catalyst effective without cocatalysts or additives. Furthermore, the overall activity of catalyst **3** is better than that of **1** and **2**. This raises the question concerning the origin of such different behavior under catalytic conditions (i.e., a pentacoordinated Ta-metallacycle species with chloride versus siloxy ligands saturating the other coordinating positions).

DFT calculations were performed to elucidate the question.[12] The guideline of this theoretical part is the mechanism of ethylene trimerization described by Houk,[7] and the similar work of Ziegler[13a] and Budzelaar[13b] on ethylene trimerization promoted by Ti catalysts. We first investigated three consecutive ethylene insertions on **3a** to form a Ta-cyclononane, which means a C8 skeleton. Ethylene coordination to **3a** is clearly an exergonic step, with **5** favored by −38.2 kcal/mol (see Figure 2) due to the high electrophilicity of the Ta^{III} center of **3a**.

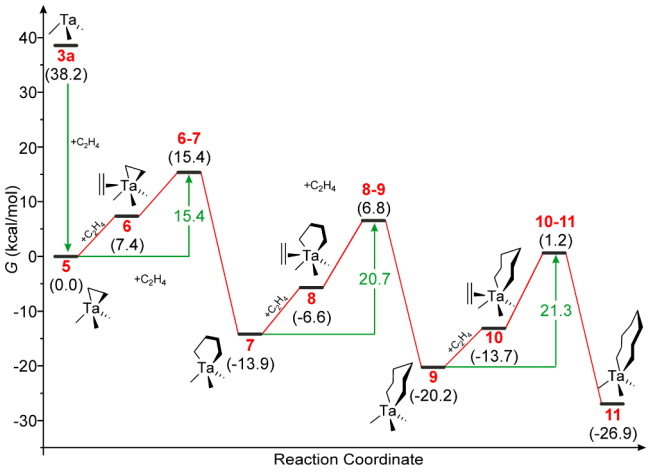

Figure 2. Energy profile for ethylene polymerization promoted by **3a**.

Using **5** as the starting point in the energy profile of Figure 2, coordination of the second ethylene unit to **6** and formation of the Ta^{V}-cyclopentane **7**, through transition state **6**−**7**, has a free energy barrier, $\Delta G^{\ddagger}_{Ins}$, of 15.4 kcal/mol, with an overall energy gain of 13.9 kcal/mol (see Figure 2). Coordination and insertion of the next ethylene molecule, to give the Ta^{V}-cycloheptane **9**, is somewhat more difficult, with a $\Delta G^{\ddagger}_{Ins}$ of 20.7 kcal/mol and an energy gain of only 6.3 kcal/mol. The final insertion step considered, leading to the C8 skeleton of the Ta^{V}-cyclononane species **11**, has a $\Delta G^{\ddagger}_{Ins}$ of 21.3 kcal/mol, with an energy gain of 6.7 kcal/mol. The similar barrier and energy gain of the second and third ethylene additions, leading to **9** and **11**, respectively, suggests that convergence in the number has been substantially achieved, and further ethylene insertion will have a free energy barrier around 20−21 kcal/mol and a free energy gain around 7 kcal/mol. The overall chemical picture emerging from Figure 2 is consistent with the similar profile reported by Houk for **1**, despite the difference between the two systems.[7]

Next, we studied the competitive chain termination mechanism from the Ta-cycloheptane species **9**, leading to a coordinated 1-hexene molecule that can be replaced by an ethylene molecule to restart the cycle. As indicated in the literature,[7,13] 1-hexene formation proceeds through a direct H-transfer from one C_β atom of **9** to the C_α atom of the other end of the Ta-cycloheptane ring (see Figure 3). According to

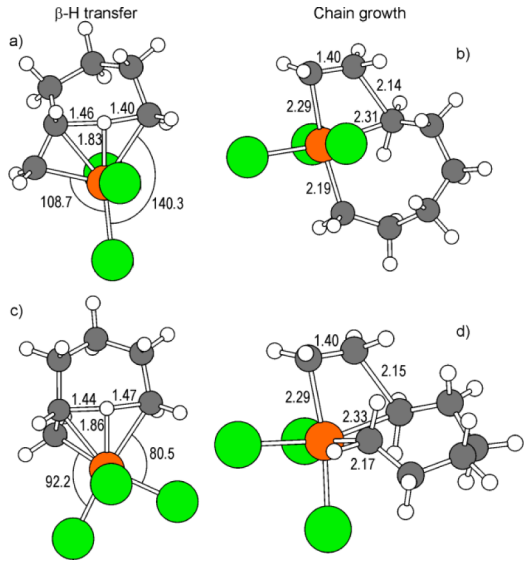

Figure 3. Transition state geometry for β-H transfer and ethylene insertion on the Ta-cycloheptane species with **1** (a and c) and **4a** (b and d); distances are in angstroms, angles are in degrees. The geometries of the analogous transition states for **2** on one side, and **3a**, **3b**, and **4b** on the other side, are extremely similar to those of **1** and **4a**, respectively and, thus, are not displayed.

calculations, this step has a free energy barrier, $\Delta G^{\ddagger}_{BHT}$, of 25.4 kcal/mol, which is 4.1 kcal/mol higher than the $\Delta G^{\ddagger}_{Ins}$ for formation of the Ta-cyclononane species (see Table 3).

Table 3. Free Energy Barrier (kcal/mol) for 1-Hexene Formation and Ethylene Insertion from the Ta-cycloheptane Intermediates

	system	$\Delta G^{\ddagger}_{Ins}$	$\Delta G^{\ddagger}_{BHT}$	$\Delta G^{\ddagger}_{BHT-Ins}$
1	$[TaCl_3]$	25.4	18.9	−6.5
2	$[(\equiv SiO)TaCl_2]$	27.1	18.5	−8.6
3a	$(\equiv SiO)_3Ta$	21.3	25.4	4.1
3b	$(\equiv SiO)_3Ta$	29.9	31.8	1.9
4a	$[TaCl_3]$	19.1	24.3	5.2
4b	$[TaCl_3]$	21.7	22.6	0.8

Therefore, calculations in agreement with experiments indicate that the Ta-cycloheptane **9** with catalyst **3a** is meant to evolve toward polymerization rather than 1-hexene formation. This is a striking difference from previous experiments on catalysts **1** and **2** and theoretical results on **1** which evidenced that the Ta-cycloheptane is more easily converted into 1-hexene rather than a long PE chain. Indeed, calculations on **1** indicated that 1-hexene formation is favored by 10.7 kcal/mol over Ta-cyclononane formation.[7]

These unexpected results led us to investigate this point in detail, since the simplicity of these self-activated systems offers a way to understand the factors that allow the switch from a trimerization to a polymerization catalyst. Catalysts **1** and **3a** differ by the replacement of the chloride ligands with siloxy ligands and by the geometrical constraint on the O−Ta−O angles in **3a**, versus a very flexible and roughly trigonal

dx.doi.org/10.1021/cs400349p | ACS Catal. 2013, 3, 1360−1364

bipyramid geometry in **1**. Therefore, we decided to examine system **2**, with a chloride replaced by a siloxy group; system **3b**, another possible geometry corresponding to a tripodal Ta-species grafted on SiO_2; and models **4a** and **4b**, with frozen Cl−Ta−Cl angles. The free energy barriers for 1-hexene formation and ethylene insertion from the corresponding Ta-cycloheptane species were calculated, and their difference, $\Delta G^{\ddagger}_{\mathrm{BHT-Ins}}$, is reported in Table 3.

According to Table 3, $\Delta G^{\ddagger}_{\mathrm{BHT-Ins}}$ is negative for **1** and **2**, which means that, in agreement with experiments, 1-hexene formation is favored. The rather similar numbers calculated for **1** and **2** indicate that substituting a chloride with a siloxy group has a minor impact on the absolute free energy barriers and, thus, also on their difference. As a remark, the siloxy moiety is best located in the equatorial plane, which explains its reduced impact on the energetics. In addition, the overall geometry is very consistent with a Ta species grafted on the silica surface, with the forming 1-hexene protruding away from the surface, consistent with the structure of the ethylene derivative of **2** shown in Figure 1.

Furthermore, the numbers reported in Table 3 indicate that for systems **3a** and **3b**, $\Delta G^{\ddagger}_{\mathrm{BHT-Ins}}$ is positive, which means that chain growth is favored over 1-hexene formation, in agreement with the experiments described above. Furthermore, the rather different $\Delta G^{\ddagger}_{\mathrm{BHT-Ins}}$ calculated for **3a** and **3b** indicates that different tripodal Ta species can yield PEs with largely different molecular masses, in agreement with the multimodal GPC curves. Finally, the rather high $\Delta G^{\ddagger}_{\mathrm{BHT-Ins}}$ calculated for **3a** is consistent with the experimental formation of a fraction of ultrahigh-molecular-mass PE. Further evidence that the different behavior of **1**−**3** is mostly a consequence of the geometrical constraint due to tripodal grafting of the catalytically active Ta atom is given by the similarity in the $\Delta G^{\ddagger}_{\mathrm{BHT-Ins}}$ calculated for **3a** and **3b** to that calculated for **4a** and **4b**, respectively. Inspection of the transition state geometry for β-H transfer and for chain growth from the Ta-cycloheptane species (see Figure 3) illuminates the origin of the different behavior.

Focusing on the transition state for β-H transfer, it assumes a trigonal bipyramid geometry in systems **1** and **2**, with the forming C═C bond and the breaking Ta-bond in equatorial positions. The C═C bond is almost perfectly in the equatorial plane, and the overall geometry is rather similar to the transition state for the β-H transfer to the monomer usually calculated as a typical termination reaction with group 4 polymerization catalysts (see Figure 3a).[14] Differently, for systems **3a**−**3b** and **4a**−**4b**, the structural constraint on the O−Ta−O and Cl−Ta−Cl angles imposes a distorted square pyramid geometry, with one Cl or O ligand in the apical position. This reduces the space available to the reacting atoms, forcing the forming C═C bond out of the basal plane (see Figure 3c), preventing the β-H transition state from assuming its typical in-plane geometry, which results in a higher barrier for 1-hexene formation. In short, the different geometry around the Ta center in **1** and **2** on one side, and **3a**−**3b** and **4a**−**4b** on the other side, is somewhat reminiscent of the different situation between group 4 metallocenes, which present a remarkably open equatorial belt that can easily accommodate the space-demanding transition state for β-H transfer to the monomer,[14] and heterogeneous Ziegler−Natta catalysts, or homogeneous bis-phenoxyimine and bis-phenoxyamine catalysts, that present an octahedral geometry with reduced space for the space demanding transition state for β-H transfer to the monomer.[15] Not surprisingly, low molecular mass is a classical weakness of metallocenes, whereas for Zielger−Natta catalysts, the polymer molecular mass is controlled by adding H_2 to the reaction media.

Moving to the transition state for chain growth, the Ta center presents an almost octahedral geometry in all systems **1**−**4**. In **1** and **2**, the forming bond is trans to a Ta−C bond (see Figure 3b), whereas in **3a**−**3b** and **4a**−**4b**, it is trans to a softer Cl ligand (see Figure 3d), which helps ethylene insertion. In addition, the geometrical distortion from trigonal bipyramid to an octahedral geometry in **1** and **2** costs energy, whereas the structural constraint on the O−Ta−O and Cl−Ta−Cl angles in **3a**−**3b** and **4a**−**4b** makes these systems ready to coordinate and insert the ethylene molecule. Indeed, the energy required to deform the trigonal bipyramid Ta-cycloheptane of **1** to the octahedral type geometry in **4a** amounts to 8.7 kcal/mol.

In conclusion, the main results achieved by the present work can be summarized as follows:

1) We demonstrated that a well-defined Ta^{III} species can promote ethylene enchainment, producing mainly linear PE, with reasonable amounts of 1-hexene and higher LAOs. This finding supports previous mechanistic studies that suggested reduction of the starting Ta^{V} precatalyst to a Ta^{III} species as an activation event.
(2) We demonstrated that the electronic impact of the ligands to the Ta species is substantially minor, since replacement of Cl atoms with siloxy ligands scarcely impacts the calculated energy profiles. This indicates that there is flexibility to try different ligand schemes to tune the performance of Ta catalysts for 1-hexene production.
(3) We demonstrated that a trigonal bipyramid geometry at the Ta center is fundamental to give enough space for the space demanding β-H transfer transition state releasing 1-hexene and, at the same time, to make difficult the geometrical deformation toward an octahedral geometry, a step required for coordination and insertion of another ethylene molecule. This indicates that work on new ligands should focus on those preserving the trigonal bipyramid geometry.

We believe that the points above rationalize well all the available experimental data on Ta-promoted ethylene trimerization and define clearly the strategies that should be used to design new Ta-based catalysts for 1-hexene formation.

■ ASSOCIATED CONTENT

Ⓢ Supporting Information

Experiment details, IR, NMR, GC, and other characterization data; full computational details; Cartesian coordinates; and energies of all the species discussed in this work. This material is available free of charge via the Internet at http://pubs.acs.org.

■ AUTHOR INFORMATION

Corresponding Author

*E-mails: (L.C.) Luigi.cavallo@kaust.edu.sa, (J.-M.B.) Jean-Marie.basset@kaust.edu.sa.

Notes

The authors declare no competing financial interest.

■ ACKNOWLEDGMENTS

We thank SABIC for the generous endowment (to J.M.B.) and for research support (to Y.C.) and the OCRF for the generous support of our studies (E.C.). We appreciate technical cooperation from KAUST, KFUPM, CRP, and CoRE-PRP.

REFERENCES

(1) (a) Whiteley, K. S. *Polyethylene: Ullmann's Encyclopedia of Industrial Chemistry*; Wiley-VCH Verlag GmbH & Co. KGaA: Weinheim, 2011. (b) Heggs, T. G. *Polypropylene: Ullmann's Encyclopedia of Industrial Chemistry*; Wiley-VCH Verlag GmbH & Co. KGaA: Weinheim, 2011.

(2) (a) Burger, B. J.; Thompson, M. E.; Cotter, W. D.; Bercaw, J. E. *J. Am. Chem. Soc.* **1990**, *112*, 1566. (b) Alelyunas, Y. W.; Guo, Z.; LaPointe, R. E.; Jordan, R. F. *Organometallics* **1993**, *12*, 544. (c) Tsutsui, T.; Mizuno, A.; Kashiwa, N. *Polymer* **1989**, *30*, 428. (d) Chien, J. C. W.; Kuo, C.-I. *J. Polym. Sci., Part A: Polym. Chem.* **1986**, *24*, 1779.

(3) (a) Bauer, R. S.; Glockner, P. W.; Keim, W.; Zwet, H. V.; Chung, H.; Shell Oil Co.; U.S. Patent No. 3644563, 1972. (b) Biagini, P.; Gila, L. Polimeri Europa SPA, Polimeri Europa SRL, Enichem SPA; European Patent No. 1453604, 2003. (c) van Leeuwen, P. W. N. M.; Clément, N. D.; Tschan, M. J.-L. *Coord. Chem. Rev.* **2011**, *255*, 1499.

(4) For ethylene polymerization, see: (a) Eisch, J. J. *Organometallics* **2012**, *31*, 4917. (b) Gibson, V. C.; Spitzmesser, S. K. *Chem. Rev.* **2003**, *103*, 283. (c) Wang, B. Q. *Coord. Chem. Rev.* **2006**, *250*, 242. and references therein. For ethylene oligomerization, see: (a) McGuinness, D. S. *Chem. Rev.* **2011**, *111*, 2321. (b) Agapie. *Coord. Chem. Rev.* **2011**, *255*, 861. (c) Skupinska, J. *Chem. Rev.* **1991**, *91*, 613 and references therein..

(5) For Ta-catalyzed ethylene polymerization, see: (a) Murtuza, S.; Harkins, S. B.; Long, G. S.; Sen, A. *J. Am. Chem. Soc.* **2000**, *122*, 1867. (b) Mashima, K.; Fujikawa, S.; Nakamura, A. *J. Am. Chem. Soc.* **1993**, *115*, 10990. (c) Bazan, G. C; Donnelly, S. J.; Rodriguez, G. *J. Am. Chem. Soc.* **1995**, *117*, 2671. (d) Rodriguez, G.; Bazan, G. C. *J. Am. Chem. Soc.* **1995**, *117*, 10155.

(6) For Ta-catalyzed ethylene oligomerization, see: (a) Andes, C.; Harkins, S. B.; Murtuza, S.; Oyler, K.; Sen, A. *J. Am. Chem. Soc.* **2001**, *123*, 7423. (b) Arteaga-Müller, R.; Tsurugi, H.; Saito, T.; Yanagawa, M.; Oda, S.; Mashima, K. *J. Am. Chem. Soc.* **2009**, *131*, 5370.

(7) Yu, Z.-X.; Houk, K. N. *Angew. Chem., Int. Ed.* **2003**, *42*, 808.

(8) Chen, Y.; Callens, E.; Abou-Hamad, E.; Merle, N.; White, A. J. P.; Taoufik, M.; Copéret, C.; Le Roux, E.; Basset, J.-M. *Angew. Chem., Int. Ed.* **2012**, *51*, 11886.

(9) (a) Neithamer, D. R.; LaPointe, R. E.; Wheeler, R. A.; Richeson, D. S.; Van Duyne, G. D.; Wolczanski, P. T. *J. Am. Chem. Soc.* **1989**, *111*, 9056. (b) Covert, K. J.; Neithamer, D. R.; Zonnevylle, M. C.; Lapointe, R. E.; Schaller, C. P.; Wolczanski, P. T. *Inorg. Chem.* **1991**, *30*, 2494.

(10) (a) Taoufik, M.; De Mallmann, A.; Prouzet, E.; Saggio, G.; Thivolle-Cazat, J.; Basset, J.-M. *Organometallics* **2001**, *20*, 5518. (b) Saggio, G.; De Mallmann, A.; Maunders, B.; Taoufik, M.; Thivolle-Cazat, J.; Basset, J.-M. *Organometallics* **2002**, *21*, 5167. (c) Soignier, S.; Taoufik, M.; Le Roux, E.; Saggio, G.; Dablemont, C.; Baudouin, A.; Lefebvre, F.; De Mallmann, A.; Thivolle-Cazat, J.; Basset, J.-M.; Sunley, G.; Maunders, B. *Organometallics* **2006**, *25*, 15769.

(11) Vidal, V.; Theolier, A.; ThivolleCazat, J.; Basset, J. M.; Corker, J. *J. Am. Chem. Soc.* **1996**, *118*, 4595.

(12) The M06 DFT calculations were performed with the Gaussian09 package using the TZVP basis set on main group atoms, and the SDD-ECP basis set on Ta. Solvent effects, toluene, were included with the PCM approach. Full details are in the Supporting Information.

(13) (a) Blok, A. N. J.; Budzelaar, P. H. M.; Gal, A. W. *Organometallics* **2003**, *22*, 2564. (b) Tobisch, S.; Ziegler, T. *Organometallics* **2003**, *22*, 5392.

(14) (a) Lohrenz, J. C. W.; Woo, T. K.; Ziegler, T. *J. Am. Chem. Soc.* **1995**, *117*, 12793. (b) Cavallo, L.; Guerra, G. *Macromolecules* **1996**, *29*, 2729.

(15) (a) Cavallo, L.; Guerra, G.; Corradini, P. *J. Am. Chem. Soc.* **1998**, *120*, 2428. (b) Seth, M.; Margl, P. M.; Ziegler, T. *Macromolecules* **2002**, *35*, 7815. (c) Talarico, G.; Busico, V.; Cavallo, L. *Organometallics* **2004**, *23*, 5989. (d) Toto, M.; Cavallo, L.; Corradini, P.; Moscardi, G.; Resconi, L.; Guerra, G. *Macromolecules* **1998**, *31*, 3431.